Optical Phase Control of Coherent Electron Dynamics in Metals

H. Petek,[1,*] A. P. Heberle,[2] W. Nessler,[1] H. Nagano,[1] S. Kubota,[1] S. Matsunami,[1] N. Moriya,[1] and S. Ogawa[1]
[1]*Advanced Research Laboratory, Hitachi Ltd. Hatoyama, Saitama 350-03 Japan*
[2]*Hitachi Cambridge Laboratory, Madingley Road, Cambridge CB30HE, United Kingdom*
(Received 8 July 1997)

The control of electron distribution excited in a metal through optical phase of the excitation light is demonstrated. Two-photon photoemission from the Cu(111) surface is excited either by a pair of ~15 fs laser pulses with a mutual delay fixed to an accuracy of ±0.025 fs, or by a single, frequency-chirped pulse. As a consequence of optical coherence in the two-photon excitation process, the photoemission spectra do not only depend on the frequency, as in conventional spectroscopy, but also on the phase of the excitation light. This may be a general phenomenon in multiphoton ionization. [S0031-9007(97)04735-2]

PACS numbers: 73.50.Gr, 78.40.Kc, 79.60.–i, 82.65.–i

The reflection of light and flow of current in response to external, time-varying fields are defining electronic properties of metals. An electromagnetic wave with a frequency $\omega < \omega_p$ (ω_p is the plasma frequency) is attenuated exponentially at the metal-vacuum interface due to the dynamical response of electrons. The field creates a microscopic polarization at the surface, which can decay by reemission of the field (reflection), or by absorption of a photon (e-h creation). According to the Drude theory, the reflection and absorption of light by a free-electron metal are described, respectively, by the real and imaginary parts of the dielectric constant, $\varepsilon(\omega) = 1 - \omega_p^2/\omega(\omega + i/\tau_0)$, where τ_0 is the optical relaxation time [1,2]. The free-carrier absorption occurs as a second-order process, where a carrier absorbs a photon and simultaneously scatters with a phonon or impurity to conserve momentum. Elastic scattering destroys the phase relation between the excitation created in the sample and the external field. Thus, τ_0 is a phenomenological dephasing time. Analysis of free-carrier absorption in noble metals shows that for visible light $\omega\tau_0 > 1$: For example, for Cu at 400 nm (3.1 eV), τ_0 is ~3.5 fs [2], while an optical cycle is 1.33 fs. Thus, the scattering processes described by τ_0 do *not* present a fundamental limit for controlling quantum dynamical response of electrons in metals by means of the optical phase.

Coherent control of quantum dynamics is a rapidly developing field of physical sciences [3]. Demonstration of control of quantum dynamics in atoms [4], molecules [5,6], molecular crystals [7], and semiconductors [8] has been achieved with phase-engineered light pulse sequences and chirped pulse excitation [3]. Interference between one- and two-photon excitation has been used for control of electrical currents in semiconductors [9] and the direction of photoemission from a surface [10]. Optical control of electron dynamics in metals and at metallic interfaces also is of great interest in a variety of fields including solid state physics, surface science, and for applications in optoelectronics. However, the dephasing time implied by τ_0, which is less than the currently available laser pulse widths, seems to impose severe limits for demonstration and application of coherent control in metals. Nevertheless, development of ultrafast interferometric techniques for studying coherent dynamics [8,11] has opened the way to test the limits imposed by the Drude theory. Recent time-resolved photoemission studies of Cu(111) demonstrated that the dephasing times of electrons at metal surfaces can exceed 20 fs [10,12]. Here, optical phase control of the two-photon photoemission process in Cu(111) is demonstrated by two different methods.

Optical phase, energy, and momentum-resolved measurements of electron dynamics on <10 fs time scales are made possible by recent advances in femtosecond laser technology [13] and time-resolved photoemission techniques [11,14,15]. In interferometric two-photon time-resolved photoemission (I2PTRP), an ultrashort laser pulse (pump) incident on a metal surface couples electronic bands of the appropriate symmetry inducing a polarization at the surface [11]. This coherent excitation rapidly decays due to phase relaxation creating an incoherent, nonequilibrium distribution of charge carriers [16]. Polarization and carrier population decay is monitored by a time-delayed probe pulse induced photoemission [11,12,17].

Figure 1 shows the optical layout for I2PTRP measurements. The second harmonic light (3.1 eV) of a Ti:sapphire laser with ~15 fs pulse duration τ_p excites two-photon photoemission (2PP) from a single-crystal surface of Cu(111) under ultrahigh vacuum ($<10^{-10}$ Torr) [11,18]. Photoemitted electron current with specific kinetic energy and momentum is detected with a hemispherical energy analyzer (Vacuum Generators 100AX) operating with a nominal 25 meV resolution. Dispersion in the optical system determines the chirp (time-dependent frequency) of the pulse at the sample. Negative, zero, or positive chirp is set by translating the prism in the dispersion compensator [19]. A feedback controlled Mach-Zehnder interferometer generates phase-locked pump-probe pulse pairs (PPP) with a delay accuracy of $\pm\lambda/50$ (±0.025 fs) [8,11]. The delay either is scanned repetitively by ±100 fs and the analyzer energy is fixed to measure the interferometric two-pulse correlation (I2PC)

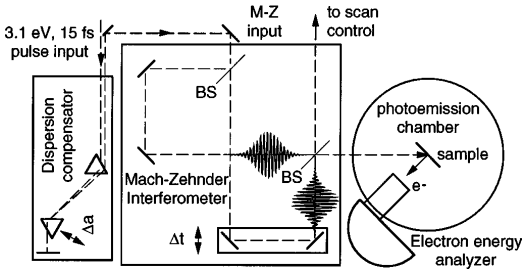

FIG. 1. Experimental setup for coherent control of 2PP. Femtosecond laser pulse width and chirp are adjusted with the dispersion compensator. Translation of the prism into/out of the beam path increases/decreases dispersion to produce an upchirped/downchirped pulse characterized by a chirp parameter a. Minimum chirp $a \approx 0$ (the shortest pulse) is set by maximizing the 2PP intensity. Generation and delay scanning of the phase-locked pulse pairs is performed with the Mach-Zehnder interferometer. The delay is controlled with a feedback system originally developed in Ref. [5], and later adopted for continuous scanning in Refs. [8] and [11]. BS indicates 50% beam splitter.

of photoemission [Fig. 2(a)] [11], or it is fixed at a specific phase delay and the analyzer energy is scanned to measure the 2PP spectra [Fig. 2(b)].

The projected band structure of Cu(111) and the excitation scheme for 2PP spectra [inset of Fig. 2(a)] shows the $L_{2'}$-L_1 band gap, which extends from -0.85 to 4.3 eV at $k_{\|} = 0$, and supports two surface states: the occupied, Shockley-type surface state (SS) at -0.39 eV [20], and an image potential state series starting with $n = 1$ state (IP) at 4.1 eV. Arrows indicate that one-photon absorption is not resonant with interband transitions that conserve momentum. In previous modeling of the 2PP process, the intermediate state was assumed to be virtual, with the IP state mostly contributing to the transition moment [11,12]. Although this mechanism is probably important near the SS $\leftrightarrow$ IP resonance [12], it cannot explain the data for chirped pulse excitation, as will be shown later. By contrast, here the intermediate state is described as a coherent superposition of all states that contribute to free-carrier absorption, and the dephasing times T_2 for the single-photon coherences are identified with the τ_0 [2]. The dephasing time for the two-photon coherence between the initial and the final state, in analogy to single-photon photoemission, is given by the Lorentzian width Γ of the SS. The width of $\sim$55 meV at 300 K implies a dephasing time ($T_2 = 2\hbar/\Gamma$) of 24 fs, which is due mainly to the hole scattering since the electron is propagating freely in the vacuum [20,21].

Interferometric two-pulse correlation measurement in Fig. 2(a) is recorded by scanning the delay while recording the 2PP signal from the SS in intervals of $\sim\lambda/14$ [11]. Optical Bloch equations, which describe the response of an atomic system to a time-varying field (time evolution of induced polarizations and populations) [19], can reproduce qualitatively the I2PC data with the present excitation scheme, or that of Ref. [11]. Simulations show that the oscillations with a period of the center frequency of the excitation light and its second harmonic, respectively,

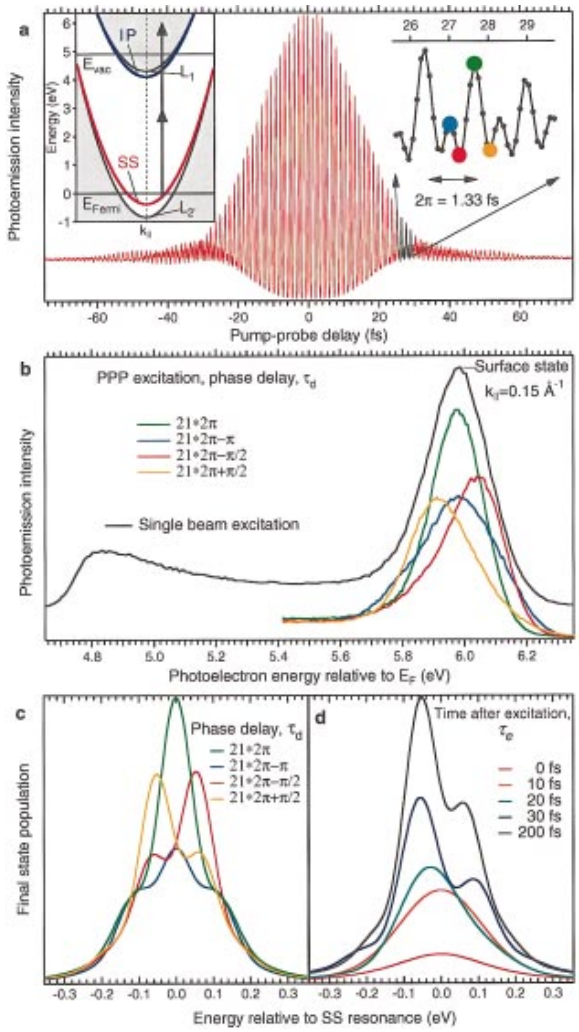

FIG. 2(color). (a) I2PC scan measured at the SS resonance and the excitation scheme for modeling the SS photoemission (inset, left). Coherence effects in the excitation process result in oscillations at the center frequency of the laser (1/1.33 fs) and its second harmonic [11]. (b) Demonstration of coherent control of two-photon photoemission. Single-pulse excitation spectrum is a reference for comparison with phase-locked pulse-pair excitation. Markers on the expanded interference fringes in (a) indicate the τ_d for measurements in (b). (c) Simulated SS spectra for the phase delays in (b). (d) Calculated time evolution of the spectrum for several values of time elapsed after excitation τ_e at $\tau_d = 21 \times 2\pi + \pi/2$.

arise from single- and two-photon coherences induced in the sample, and that their decay is consistent with dephasing due to hole scattering on a $\sim$20 fs time scale, in accordance with the photoemission linewidth measurements [11,20,21]. The observed coherence in the time domain suggests that the coherent response of the surface should also have a signature in the frequency domain. This is demonstrated in Fig. 2(b) with PPP excitation for pump-probe delays τ_d that range between 27.4–28.4 fs corresponding to approximately 21 optical cycles (phase delay is incremented from $21 \times 2\pi - \pi$ in steps of $\pi/2$, i.e., $\sim$0.33 fs). Simulation of the spectra in Figs. 2(c) and 2(d) is discussed following the results on chirped pulse

excitation. When the PPP are in phase ($\tau_d = 21 \times 2\pi$), the SS peak has *maximum* intensity and is *narrower* than the single pulse reference spectrum. By contrast, when the delay is reduced by 0.66 fs (π–out-of-phase excitation), the SS peak intensity is *minimum* and its width is *maximum*. Finally, the SS intensity is intermediate and the peak shifted to *lower* (*higher*) final state energy for $\tau_d = 21 \times \pi + \pi/2(-\pi/2)$. The phase induced changes in the 2PP reflect the Fourier transform of the electric field of the pulse pair, i.e., the spectrum. The effect of the phase on the spectra may be due to optical interference in the Mach-Zehnder interferometer when $\tau_d \leq \tau_p$, or the quantum interference in the sample when τ_d is comparable to the dephasing time. Since the intensity of the bulk bands [the pedestal below the SS in Fig. 2(b)] is not influenced by the phase, the effect cannot be due to optical interference in the interferometer, and can only be attributed to the coherent response of the Cu(111) surface. This demonstrates that the intensity and energy distribution in 2PP spectra can be manipulated through the optical phase of electric field of the excitation light.

Coherent control of 2PP also is demonstrated with chirped pulse excitation. Figure 3(a) presents a series of 2PP spectra with single pulse excitation for different values of the chirp, which is calculated from the optical constants of fused silica [19]. The amount of glass in the optical path determines the frequency chirp and width, but *not* the spectrum of the excitation pulse. The position of the SS peak in the 2PP spectra is blueshifted (redshifted) from the position of the unchirped peak by a maximum of ~50 meV for up (down) chirp produced by 1 mm translation ($a = 2.4$) of the prism into (out of) the optical path (see Fig. 1). Further translation of the prism decreases the SS peak shift.

The spectra in Figs. 2 and 3 are simulated by the optical Bloch equation method [11,19] assuming the excitation scheme in Fig. 2. The spectra are calculated by integrating the final state population over time for specific excitation fields. The final state energy is varied in discrete steps to construct a spectrum [12]. Although many aspects, such as many-body carrier interactions and realistic band structure of copper are not included, the simulation, nevertheless, provides a qualitative description for the multiphoton excitation process. Figure 2(c) shows the simulated SS spectra for delays in Fig. 2(b) using the dephasing times implied by the SS width and $\tau_0 = 10$ fs [11,20]. The calculated spectra qualitatively reproduce the experimental intensity and frequency shift patterns. Better agreement can be obtained by treating the intermediate state as a continuum rather than as a single discrete state, and by convoluting the spectra with the instrumental resolution function (~80 meV).

Several calculations also are performed on the time evolution of the spectra [Fig. 3(d)] to clarify how the optical phase affects the intensity and energy distributions in PPP excitation. The final state distributions for $\tau_d = 21 \times 2\pi + \pi/2$ in Fig. 2(d) are calculated for several values of τ_e, the time elapsed after the center of the pump pulse has interacted with the surface. For interaction times where $0 \leq \tau_e$, the final state width is significantly broader than the bandwidth of the excitation pulses due to the energy-time uncertainty. Energy is conserved as the excitation progresses by stimulated emission (reflection) or by inelastic collisions. The final state generation is retarded and depends not only on the instantaneous light field and induced excitation, but also on earlier times [22]. When $\tau_d \neq 0$, the relative phase of the pump-probe pair for each frequency component comprising the excitation light will depend on τ_d (the frequency components with the same phase will be separated by $1/\tau_d$). The in-phase frequency components will add constructively in the sample (enhanced two-photon absorption), while the out-of-phase components will add destructively (stimulated reflection). For $\tau_e \geq 20$ fs, Fig. 2(d) shows a spectral shift with respect to the single pulse energy of the SS peak as a result of constructive and destructive interference below and above the SS resonance, respectively. The depth of the modulation across the spectrum is governed by the dephasing time, i.e., the uncertainty broadening.

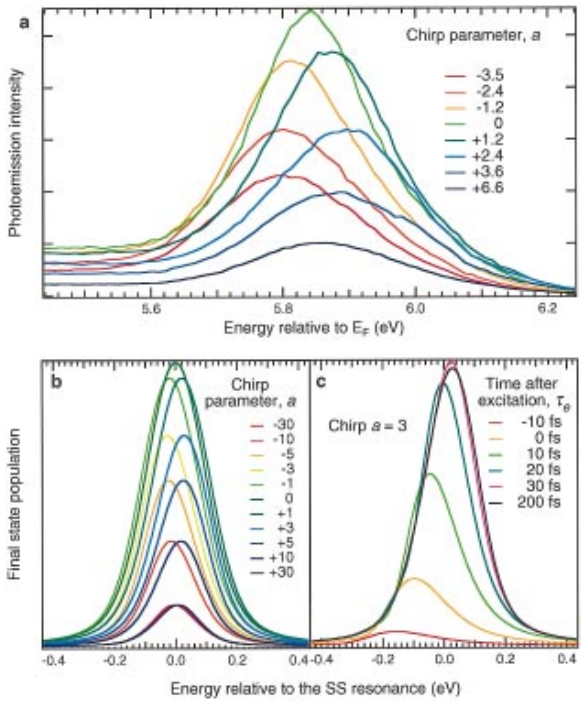

FIG. 3(color). (a) Two-photon photoemission spectra as a function of the chirp parameter a. (b) Simulation of the spectra in (a). (c) Calculated time evolution of the SS spectrum for $a = 3$.

2PP spectra also are simulated for chirped pulse excitation, where the electric field is given by $E(t) = E(a)\exp[-(t/\tau_g)^2]\cos[(\omega_l + bt)t]$. The pulse has a time-dependent frequency given by $\omega(t) = \omega_l + b \times t$, where ω_l is the center frequency. The dispersion in the optical system affects mainly the linear chirp, where $b = [a/(1 + a^2)](1/\tau_{g0}^2)$ is a constant. $E(a) = E_0(1 + a^2)^{-1/4}$ is the electric field amplitude, and

$\tau_g = \tau_{g0}(1 + a^2)^{1/2}$ is the pulse width. E_0 and τ_{g0} are the amplitude and width of a transform limited Gaussian pulse, where $a = 0$. The chirp parameter a is negative (positive) for a downchirped (upchirped) pulse. The maximum rate of change of instantaneous frequency occurs for $|a| = 1$. The chirp changes with width and amplitude of the electric field envelope of the pulse, but *not* its energy or spectrum.

The calculated 2PP spectra in Fig. 3(b) qualitatively reproduce the shift of the SS with a. The simulations show that the peak shift occurs only when the frequency of the excitation pulse is changing rapidly on the time scale of dephasing of single-photon resonances. If the spectra are calculated with the nonresonant scheme in Ref. [11], the lifetime of the virtual intermediate state is <1 fs, since the laser is detuned by 1.4 eV from the SS $\leftrightarrow$ IP resonance. This is too short to reproduce the SS shifts. The simulation gives the best agreement with the experimental shift if the two-photon excitation proceeds *via* the indirect, intraband absorption process, described above, with $\tau_0 \sim 10$ fs. A greater value of τ_0 than implied by the analysis of free-carrier absorption in copper [2] is consistent with exponential damping of the SS charge density in the bulk, and, thus, weaker coupling to the lattice [12,20].

For a more intuitive understanding of the relationship between the frequency shift and the chirp, several spectra are calculated as a function of τ_e for an upchirped pulse [Fig. 3(c)]. The rising edge of the pulse excites a highly asymmetric, redshifted, and broad spectrum, reflecting the frequency-time structure of the pulse and the uncertainty principle. The spectrum narrows with τ_e to conserve energy. However, since the instantaneous frequency increases with time, the narrowing occurs by stimulated reflection on the red edge and enhanced two-photon absorption on the blue edge. If the intermediate state is virtual, the decay of single-photon coherences is too fast compared to the change in the instantaneous frequency for the interplay between reflection and absorption to cause a spectral shift. Although there are some similarities in how the PPP and the chirped pulse excitation influence the final state distributions, a distinct difference between the two approaches to coherent control is that the Fourier transform of $E(t)$ (the spectrum) for PPP excitation depends on τ_d, but *not* on the chirp.

The 2PP spectra clearly demonstrate that the optical phase can influence electron distribution in the two-photon excitation process, despite dephasing induced by strong Coulomb interactions among the charge carriers and scattering by phonons and impurities. Coherent control of electron dynamics in metals and metallic interfaces may be applied to other phenomena involving the flow of charge on atomic scale, for instance, the charge transfer between a metal surface and adsorbed molecules or the tunneling current in scanning tunneling microscopy. Besides demonstrating the coherent control in metals, the present work also is more generally applicable. Since the optical Bloch equations are most appropriate for atomic systems, the observed effects also should occur in atoms, molecules, and semiconductors.

This work was supported in part by NEDO Joint International Research Project on Photon and Electron Controlled Surface Processes.

Note added.—Recent observation of quantum coherence in two-photon photoemission of high-lying image potential states on Cu(111) surface suggests that coherent control of electrons at metal surfaces can be extended to picosecond time scales [23].

*Corresponding author.

[1] W. P. Dumke, Phys. Rev. **124**, 1813 (1961).
[2] P. B. Johnson and R. W. Christy, Phys. Rev. B **11**, 1315 (1974); J. B. Smith and H. Ehrenreich, Phys. Rev. B **25**, 923 (1982).
[3] M. Shapiro and P. Brumer, J. Chem. Soc. Faraday Trans. **93**, 1263 (1997); W. S. Warren, H. H. Rabitz, and M. Dahleh, Science **259**, 1581 (1993); B. Kohler *et al.*, Acc. Chem. Res. **28**, 133 (1995); H. Kawashima, M. M. Wefers, and K. A. Nelson, Annu. Rev. Phys. Chem. **46**, 627 (1995).
[4] M. M. Wafers, H. Kawashima, and K. A. Nelson, J. Chem. Phys. **102**, 9133 (1995).
[5] N. F. Scherer *et al.*, J. Chem. Phys. **95**, 1487 (1991).
[6] B. Kohler *et al.*, Phys. Rev. Lett. **74**, 3360 (1995).
[7] H. Kawashima and K. A. Nelson, J. Chem. Phys. **100**, 6160 (1994).
[8] A. P. Heberle, J. J. Baumberg, and K. Köhler, Phys. Rev. Lett. **75**, 2598 (1995); A. P. Heberle *et al.*, IEEE J. Sel. Top. Quantum Electron. **2**, 1 (1996).
[9] G. Kurizki, M. Shapiro, and P. Brumer, Phys. Rev. B **39**, 3435 (1989); E. Dupont *et al.*, Phys. Rev. Lett. **74**, 3596 (1995); R. Atanasov *et al.*, Phys. Rev. Lett. **76**, 1703 (1996).
[10] N. B. Baranova, A. N. Chudinov, and B. Ya. Zel'dovich, Opt. Commun. **79**, 116 (1990).
[11] S. Ogawa *et al.*, Phys. Rev. Lett. **78**, 1339 (1997).
[12] T. Hertel *et al.*, J. Vac. Sci. Technol. A **15**, 1503 (1997).
[13] M. T. Asaki *et al.*, Opt. Lett. **18**, 977 (1993).
[14] R. Haight, Surf. Sci. Rep. **21**, 275 (1995).
[15] C. A. Schmuttenmaer *et al.*, Phys. Rev. B **50**, 8957 (1994).
[16] K. L. Kleiver, Surf. Sci. **101**, 57 (1980).
[17] S. Ogawa, H. Nagano, and H. Petek, Phys. Rev. B **55**, 10 869 (1997).
[18] S. Ogawa and H. Petek, Surf. Sci. **357–358**, 585 (1996).
[19] J.-C. Diels and W. Rudolph, *Ultrashort Laser Pulse Phenomena* (Academic Press, San Diego, 1996).
[20] B. A. McDougall, T. Balasubramanian, and E. Jensen, Phys. Rev. B **51**, 13 891 (1995); R. Matzdorf, Appl. Phys. A **63**, 549 (1996).
[21] I. Bartos and J. Koukal, Surf. Sci. **138**, L151 (1984).
[22] T. Kuhn and F. Rossi, Phys. Rev. B **46**, 7496 (1992).
[23] U. Höfer *et al.*, Science **277**, 1480 (1997); W. Plummer, Science **277**, 1447 (1997).